JOURNAL OF Materials CHEMISTRY

Crystal chemistry and redox behaviour of perovskite-related bismuth strontium calcium oxides

Claudia C. Luhrs,[a] Fernando Sapiña,[b] Daniel Beltrán-Porter,[b] Nieves Casañ-Pastor[a] and Amparo Fuertes*[a]

[a]*Institut de Ciència de Materials de Barcelona (C.S.I.C.), Campus U.A.B., 08193 Bellaterra, Spain*

[b]*Institut de Ciència de Materials de la Universitat de València, Dr. Moliner 50, 46100 Burjassot, Spain*

The synthesis and characterization of two solid solutions in the Bi–Sr–Ca–O system are reported. They have the same cationic stoichiometry but different oxygen content. The so-called oxidized solid solution $(Sr_{2-x}Ca_x)(Bi_{1.4}Ca_{0.6})O_6$ exists for $0 \leqslant x \leqslant 0.5$. The cell parameters for the member with $x=0$ are $a_o=5.89228(9)$, $b_o=5.98928(8)$, $c_o=8.38336(14)$ Å, $\beta_o=89.946(5)^\circ$, and the space group is $P2_1/n$. It shows a slightly distorted perovskite structure with parameters $\sqrt{2}a_p \times \sqrt{2}a_p \times 2a_p$ and two crystallographically independent B positions with occupancies 95% Bi/5% Ca (site 1) and 45% Bi/65% Ca (site 2) ordered in a 3D NaCl-type arrangement. The reduced solid solution, $(Sr_{2-x}Ca_x)(Bi_{1.4}Ca_{0.6})O_{6-\delta}$ ($\delta=0.79$), exists for the same cationic range and can be obtained from the oxidized solid solution by reduction in air or oxygen at 800 °C. This process is reversible: the reduced solid solution leads to the oxidized one by treatment in oxygen at 650 °C. At lower temperatures other oxidation–reduction reactions take place without apparent modification of the structure of the starting phases showing oxygen non-stoichiometry. The reduced solid solution shows a perovskite-related structure with cell parameters for $x=0$: $a_r=11.2396(5)$, $b_r=5.9097(3)$, $c_r=20.0787(9)$ Å, $\beta_r=101.747(4)^\circ$ in space group $P2_1/c$; 63.6% of bismuth is in the +3 valence state and 36.4% is in the +5 valence state.

The crystal chemistry of ternary or pseudoternary bismuth and lead oxides is relevant for the understanding of superconductivity at high temperatures in these materials. Potassium doped $BaBiO_3$ and bismuth doped $BaPbO_3$ show critical temperatures of 30 and 13 K,[1,2] respectively and have been extensively studied. $BaPb_{1-x}Bi_x0_3$ shows metallic conductivity for $0 \leqslant x \leqslant 0.35$ and semiconducting behavior for $0.35 \leqslant x \leqslant 1$. Superconductivity occurs in the metallic phase, with an optimal superconducting transition temperature at $x=0.25$. The solid solution shows orthorhombic or tetragonal symmetries for low bismuth contents and a monoclinic distortion for compositions close to $BaBiO_3$.[3] In the undoped monoclinic $BaBiO_3$ ($a=6.02$, $b=6.07$, $c=8.50$ Å, $\beta=90.2^\circ$), bismuth is present with a formal oxidation state of +4, being disproportionated into Bi^{3+} and Bi^{5+} because of the instability of the $6s^1$ configuration. The two cations occupy two crystallographically independent B positions of the perovskite that alternate along the three directions of the cubic subcell. This order, implying charge localization, results in a charge density wave phase with insulating properties.[4,5] Potassium doping induces charge delocalization that competes with the charge density wave mechanism, leading to a transition to a cubic superconducting phase for $x=0.4$. The discovery of superconductivity in $Ba_{1-x}K_xBiO_3$ took place after the finding of high T_c superconductivity in $La_{2-x}Ba_xCuO_4$ in 1986.[6] With the aim of comparing bismuth or lead perovskites with cuprates, subsequent research was done to find layered phases of the Ruddlesden–Popper type with formulation $(BaO)(BaMO_3)_n$ (M = Pb, Bi). Thus, the phases Ba_2PbO_4 and $Ba_4Pb_3O_{10}$[7,8] have been isolated and correspond to the members with $n=1$ and $n=3$ of the above series, whereas only the phase with $n=2$, $Ba_{3-x}K_xBi_2O_7$, has been found in the case of bismuth.[9] Attempts to obtain the $n=1$ and $n=3$ lead phases superconducting have been made[8,10] by doping with bismuth, but only the phase $Ba_{1.9}K_{0.1}Bi_{0.85}Pb_{0.15}O_4$ seems to be a superconductor with $T_c=14$ K.[11] The composition 'Ba_2BiO_4' does not show the K_2NiF_4 structure, corresponding in fact to perovskites with disordered barium and bismuth occupying both A and B sites. These phases show a very rich redox behaviour and crystal chemistry because of the capability of bismuth to present oxidation states of +3 and +5 with unusual coordination surroundings (for Bi^{III}).[12,13] In the bismuth-rich region of the Ba–Bi–O system, the same feature leads to the existence of a wide homogeneity range for the perovskite structure, with different superstructures depending on the temperature.[14]

Bismuth ternary oxides containing alkaline-earth ions other than barium have been studied as secondary phases in the Bi–Sr–Ca–Cu–O system, where the superconductors $Bi_2Sr_2CaCu_2O_8$ and $Bi_2Sr_2Ca_2Cu_3O_{10}$ with important technological applications belong. Phases with compositions $Ca_6Bi_6O_{15}$, $CaBi_2O_4$, $Ca_4Bi_6O_{13}$ and $Sr_2Bi_2O_5$ have been fully characterised and none of them show a structure apparently related to perovskite.[15–20] Only three phases have been found showing this structure but not superconductivity, these being $Sr_{10}Bi_6O_{24-y}$, $Sr_6Bi_2O_{12-y}$[21] and $(Ba_{1-x}Sr_x)_2(Sr_{0.67}Bi_{0.33})(Pb_{1-y}Bi_y)O_{6-\delta}$.[22] In the system Bi–Sr–Ca–O several phases ($Bi_9Sr_{11}Ca_5O_y$, $Bi_2Sr_{1-x}Ca_{1+x}O_y$, $Bi_2Sr_{3-x}Ca_xO_y$, $BiSr_{3-x}Ca_xO_y$) have been identified as impurities during the processing of high-temperature superconductors[23–25] and their stability and stoichiometry range has been recently determined.[24,25] Nevertheless, their true stoichiometry is not clear and none of them has been structurally characterised, even though proposals for their space groups have been reported. Here, we present a crystallochemical study of the oxidized and reduced forms of $Bi_9Sr_{11}Ca_5O_y$, a phase with a structure related to perovskite, and for which we propose a different formulation, $Sr_{2-x}Ca_xBi_{1.4}Ca_{0.6}O_{6-\delta}$.

Experimental

Synthesis

Samples of composition $Sr_{2-x}Ca_{0.6+x}Bi_{1.4}O_{6-\delta}$ with $\delta=0.8$ and $x=0$, 0.2, 0.4, 0.5, 0.6 and 0.7 were prepared by the ceramic

method, starting with Bi_2O_3 (Aldrich 99.9%), $SrCO_3$ (Baker 99.9%) and $CaCO_3$ (Baker 99.95%). Stoichiometric amounts of the above reactants were mixed and ground in an agate mortar, pelletized and treated in flowing synthetic air (80% O_2–20% N_2, Carburos Metálicos, 99.995%) at 800 °C for 120 h with four intermediate regrindings. The oxidized samples ($\delta=0$) were prepared by heating the corresponding reduced ones in pure flowing oxygen (Carburos Metálicos, 99.995%), with one thermal cycle of 12 h and two of 24 h at 650 °C. The heating and cooling rates in all the treatments were 200 and 300 °C min^{-1}, respectively. The purity of the samples was tested systematically by conventional X-ray diffraction and by electron diffraction combined with X-ray energy-dispersive analysis (XEDS).

Chemical analysis

Iodometric analyses were performed to determine the oxidation state for bismuth. After dissolving the samples in 3 M HCl, an excess of KI was added. The I_2 formed by reaction with Bi^V was titrated with standardized $Na_2S_2O_3$ using starch as indicator. The estimated error for these analysis is ±0.05 O per formula unit.

Thermogravimetry

The experiments were performed in a TGA-7 Perkin Elmer thermal balance (max. sensitivity = 0.1 μg) with starting sample masses of 20–40 mg and 60 cm^3 min^{-1} flow rates for purging gases. Oxygen contents determinations were attempted in Ar–H_2 (95% Ar–5% H_2, Carburos Metálicos 99.995%). The samples were heated at 15 °C min^{-1} up to 485 °C, where a 400 min isothermal step was performed. Higher temperatures were avoided in order to prevent evaporation of metallic bismuth, which becomes significant above 540 °C. The presence of small amounts of carbonates, basic carbonates or hydroxides as impurities formed in some samples by ambient exposure made those experiments unreliable from a quantitative point of view. However they were still useful to observe the relative changes on oxygen stoichiometry. Experiments under flowing oxygen or argon (Carburos Metálicos 99.995%) were performed in both non-isothermal and isothermal conditions using different maximum temperatures between 650 and 900 °C.

Electron diffraction

Electron diffraction patterns were obtained using a JEOL JEM-1210 microscope operating at 120 kV, equipped with a side-entry 60/30 ° double tilt GATHAN 646 analytical specimen holder and a Link QX2000 XEDS element analysis system. The specimens for electron microscopy were prepared by grinding the powder sample, dispersing it in *n*-butanol, and depositing a droplet of this suspension on a carbon coated holey film supported on an aluminium grid.

For quantitative XEDS analysis the specimen was held at the optimum degree of tilt with respect to the X-ray detector, $x=+20°$, $y=-20°$. We used the ratio method on thin crystals.[26,27] Typically, 20 small crystals of each phase, showing their characteristic electron diffraction patterns, were analysed at 100 000 × with a counting time of 100 s. The proportionality constants were determined by analysing pure standard samples of $Bi_2Sr_2O_5$ and $CaBi_2O_4$.[16,19]

X-Ray diffraction

X-Ray powder diffraction patterns were obtained using Cu radiation with both a Siemens D-500 diffractometer [λ(Cu-Kα) = 1.5418 Å] and a Rigaku Rotaflex RU-200B rotating-anode diffractometer featuring monochromatized (Ge 111) radiation [λ(Cu-Kα_1) = 1.5406 Å]. The patterns for routine phase identification and purity checking of the samples were collected between $2\theta=5$ and 70 ° with a step size of 0.04 ° and a scan speed of 4 ° min^{-1} in 2θ. The data for the refinement of cell parameters were collected with a step size of 0.02 °. The pattern for the crystal structure determination of $Sr_2(Ca_{0.6}Bi_{0.4})BiO_6$ was obtained with the Rigaku diffractometer between $2\theta=15$ and 115 °, with step size of 0.02 ° and a counting time of 12 s. Profile refinements, using the Rietveld method, were carried out with the help of program FULLPROF.[28]

Magnetic susceptibility

Magnetic measurements were performed at 5 K with a Quantum Design SQUID magnetometer for magnetic fields of 10, 100, 1000 and 10 000 G. Electrical resistivity measurements were done by using the four-point method (1 mA) at room temperature.

Results

In the course of our work on new tubular phases related to the $Bi_2Sr_2Ca_{n-1}Cu_2O_{2n+4}$ high-temperature superconductors[29–31] the systematic presence in powder samples of crystals of composition close to $SrBi_{0.7}Ca_{0.3}O_y$ as determined by XEDS and characteristic electron diffraction pattern (see below) was observed. The synthesis of that phase was then tackled assuming the formulation $Bi_{1-x}Ca_xSrO_y$ ($0\leqslant x\leqslant1$) and single-phased samples were obtained only for $x=0.3$. The oxygen content was determined by iodometric analysis allowing the formulation of the stoichiometry $SrBi_{0.7}Ca_{0.3}O_{2.6}$. In order to investigate the relative variation of the alkaline-earth metal content the preparative work was extended under the $(Sr_{2-x}Ca_x)(Bi_{1.4}Ca_{0.6})O_{6-\delta}$ stoichiometry constraint. The samples were routinely characterized by powder X-ray (XRD) and selected area electron diffraction (SAED) and their composition was analysed by XEDS and TG. The limit of the solid solution involving the formal substitution of calcium for strontium was found to be $x\approx0.5$. The oxygen content of the samples, determined from iodometric analysis was 5.20 ± 0.05.

Annealing experiments under pure oxygen at low temperature showed that all the samples of this solid solution gain the same amount of oxygen, up to $\delta=0$, independently of the Sr/Ca ratio. The resulting oxidized compounds are single-phased with characteristic XRD and SAED patterns, indicating that a solid solution, $(Sr_{2-x}Ca_x)(Bi_{1.4}Ca_{0.6})O_6$, exists at least in the same stoichiometry range that the original reduced one. Fig. 1 shows the XRD patterns of the $x=0$ member of each phase, the reduced $Sr_2Bi_{1.4}Ca_{0.6}O_{5.21}$ (*a*), and the oxidized one, $Sr_2Bi_{1.4}Ca_{0.6}O_6$ (*b*).

Redox behaviour and phase identification

The reduction of $Sr_2Bi_{1.4}Ca_{0.6}O_{6-\delta}$ in Ar/H_2 (Fig. 2) takes place in two well separated steps. The total mass loss is 8.13% (implying $\delta=0.45$) and corresponds to the overall process:

$$Sr_2Bi_{1.4}Ca_{0.6}O_{6-\delta}+(3.4-\delta)H_2$$
$$\rightarrow 2SrO+0.6CaO+1.4Bi+(3.4-\delta)H_2O$$

This δ value is significantly lower than that obtained by iodometric analysis (0.79 ± 0.05). The oxidation of a different sample with $x=0$ in O_2 in isothermal conditions (see inset of Fig. 3), gave a δ value of 0.78 if the uptake of oxygen is assumed to be up to $\delta=0.0$ (from iodometric analysis, this δ was 0.02, near zero, for a sample prepared in the furnace in the same conditions). The low δ value obtained in Ar–H_2 for the first sample could be due to a larger than expected mass loss caused by the presence of small amounts of carbonates, basic carbonates or hydroxides formed during atmospheric exposure. The estimated error in the oxygen content caused by the hypothetical presence of these products, is important for TG and negligible for iodometric analysis. Because of that,

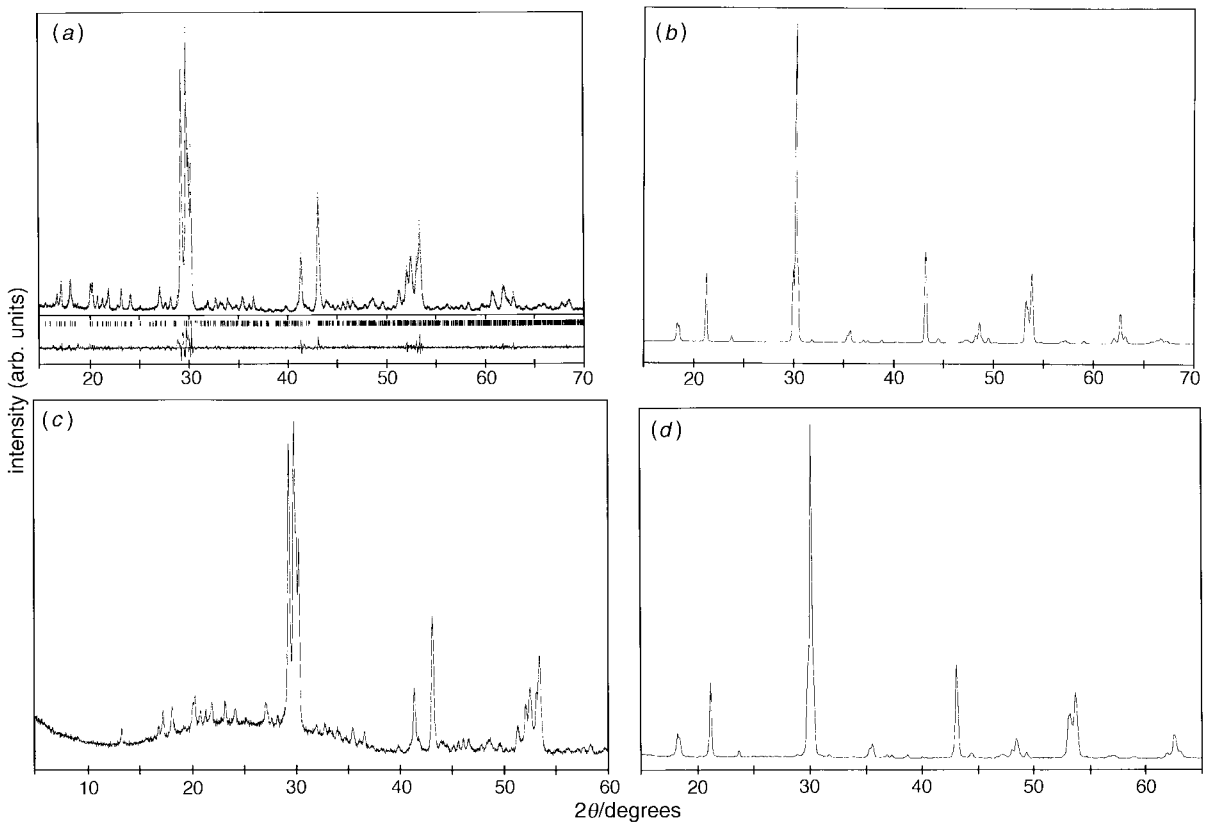

Fig. 1 Powder X-ray diffraction pattern of (*a*) $Sr_2Bi_{1.4}Ca_{0.6}O_{6-\delta}$, $\delta=0.79$; (*b*) $Sr_2Bi_{1.4}Ca_{0.6}O_6$; (*c*) $Sr_2Bi_{1.4}Ca_{0.6}O_{4.70}$, (*d*) $Sr_2Bi_{1.4}Ca_{0.6}O_{5.60}$. (*a*) includes the peak fitting performed with the program FULLPROF.

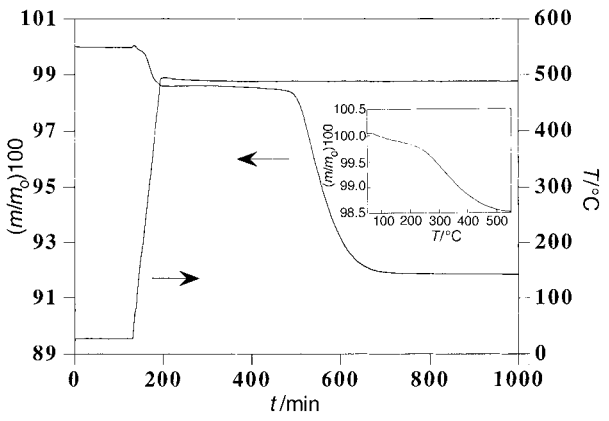

Fig. 2 TG plot in $Ar-H_2$ for $Sr_2Bi_{1.4}Ca_{0.6}O_{6-\delta}$ ($\delta=0.79$)

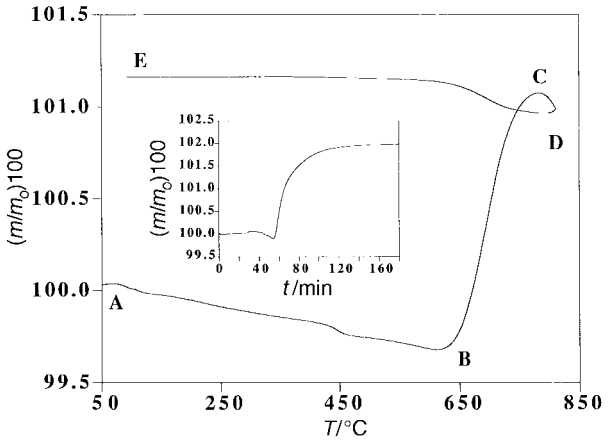

Fig. 3 TG plot in O_2 for $Sr_2Bi_{1.4}Ca_{0.6}O_{6-\delta}$ ($\delta=0.79$). Inset: isothermal run performed at 650 °C.

we have taken $\delta=0.79$ as the true oxygen content for this phase and have corrected the δ values obtained by TG for the intermediate phase with lower oxygen content.

The first mass loss in $Ar-H_2$ (Fig. 2), 1.43%, occurs from 248 °C (onset) up to 550 °C (see the non isothermal run on the inset) and could be associated with the stabilization of a phase with stoichiometry $Sr_2Bi_{1.4}Ca_{0.6}O_{4.70}$. Fig. 1(*c*) shows the XRD pattern of this phase, prepared by treatment of $Sr_2Bi_{1.4}Ca_{0.6}O_{5.21}$ in $Ar-H_2$ at 485 °C. The second step in the TG experiment takes place after isothermal treatment at 485 °C and corresponds to the decomposition of the phase with 4.70 O. The stoichiometry obtained for the sample, $Sr_2Bi_{1.4}Ca_{0.6}O_{5.21}$, leads to an average formal oxidation state for bismuth of +3.73, *i.e.*, a content of 36.4% of Bi^V and 63.6% of Bi^{III}. The TG in oxygen for the same sample (Fig. 3) shows an initial small mass loss (from A to B). This could be assigned to CO_2 or H_2O losses from the mentioned impurities that may be present in the sample. At 650 °C a mass gain takes place, finishing at 782 °C (point C). At higher temperatures (800 °C) the sample loses 0.2 mass% that is partially recovered when cooling to room temperature (from D to E). The stoichiometry in C is $Sr_2Bi_{1.4}Ca_{0.6}O_{6.00}$, as determined with the isothermal run at 650 °C depicted in the inset of Fig. 3 and iodometric analysis, corresponding to a formal oxidation state for bismuth of +4.85 (92.5% of Bi^V and 7.5% of Bi^{III}). The starting reduced phase, $Sr_2Bi_{1.4}Ca_{0.6}O_{6-\delta}$ ($\delta=0.79$), is pale yellow, whereas the oxidized sample, $Sr_2Bi_{1.4}Ca_{0.6}O_{6.00}$, is greenish black. This behaviour is similar for every sample in the reduced solid solution.

The powder X-ray diffraction pattern of the sample $Sr_2Bi_{1.4}Ca_{0.6}O_{5.21}$ [Fig. 1(*a*)] shows numerous peaks of low intensity, the more important being centred at 2θ *ca.* 30, 40–45 and 50–55°. Perovskites show their more intense peaks in these ranges and therefore this phase could have a structure related to them. The electron diffraction patterns along the [100], [010] and [001] zone axes (Fig. 4), and others planes obtained by tilting around the *b** axis, can be indexed on the

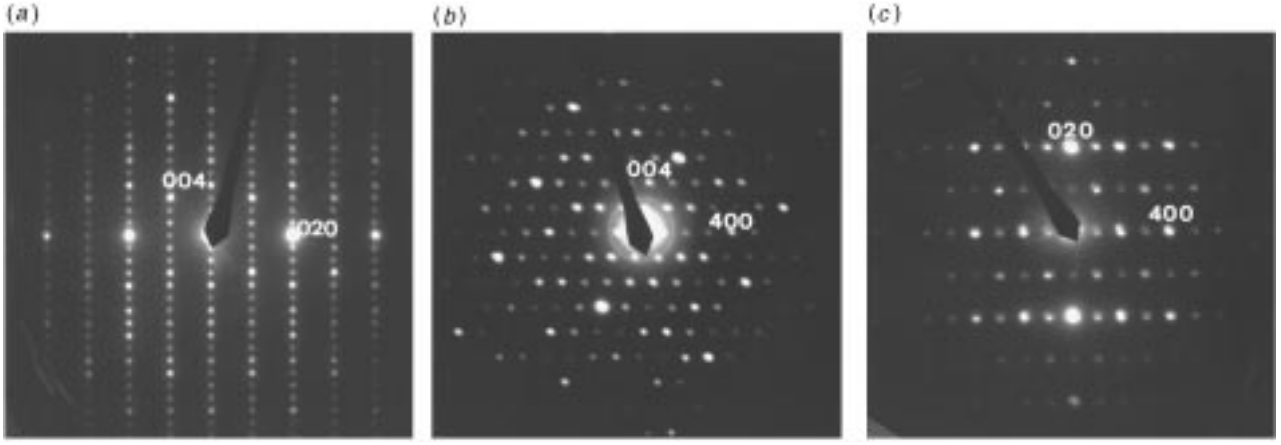

Fig. 4 Electron diffraction patterns along the [100] (*a*), [010] (*b*) and [001] (*c*) zone axes of $Sr_2Bi_{1.4}Ca_{0.6}O_{5.21}$

basis of a monoclinic cell with $a=11.2$, $b=5.9$, $c=20.0$ Å and $\beta=102^\circ$. Reflection conditions $h0l$, $h=2n$, $00l$, $l=2n$, and $0k0$, $k=2n$, are in agreement with the $P2_1/c$ space group (no. 14).[32] The spots $00l$ with $l=2n+1$ in the pattern along the [100] zone axis are due to multiple reflection. The relationship of this cell with the perovskite subcell may be obtained taking into account the following considerations: (*i*) the electron diffraction pattern along the $[60\bar{1}]$ zone axis (Fig. 5) could correspond to the $[110]_p$ plane of a perovskite subcell with axes $a_s \approx b_s = \sqrt{2}a_p \approx 6$ Å, $c_s = a_p$ [a_p being the parameter of the ideal cubic perovskite cell (*ca.* 4 Å)]; (*ii*) in the a^*c^* plane it is possible to distinguish some intense reflections that are indexed 504 and $\bar{1}06$ (Fig. 6). These reflections define a subcell of dimensions 2.9×2.2 Å with orthogonal axes, that would correspond to a perovskite with parameters $a_s = \sqrt{2}\ a_p$ and $c_s = a_p$. These two axes form angles, in the reciprocal space, of 25.5 and 15.5° with a^* and c^*, respectively. Then the cell $11.2 \times 5.9 \times 20$ Å is a supercell of a perovskite cell with $a_s = \sqrt{2}\ a_p$, $b_s = \sqrt{2}\ a_p$ and $c_s = a_p$, both having the b axis in common. The lattice parameters were determined by a peak fitting of the X-ray powder diffraction data using the FULLPROF program[28] to $a=11.2396(5)$, $b=5.9097(3)$, $c=20.0787(9)$ Å and $\beta=101.747(4)^\circ$ [see Fig. 1(*a*)].

The phase with stoichiometry $Sr_2Bi_{1.4}Ca_{0.6}O_{4.70}$, obtained by reduction of $Sr_2Bi_{1.4}Ca_{0.6}O_{5.21}$ in $Ar-H_2$ (see before), shows similar X-ray and electron diffraction patterns and cell parameters [Fig. 1(*c*)]. However, it is possible to observe satellite reflections in the electron diffraction plane along the direction indexed $[110]_p$ in the perovskite subcell (see Fig. 7). These satellites could be related to oxygen vacancies additional to those existing in the phase with 5.21 O that would lead to the appearance of an incommensurate superstructure. The average formal valence for bismuth in this phase is +3.

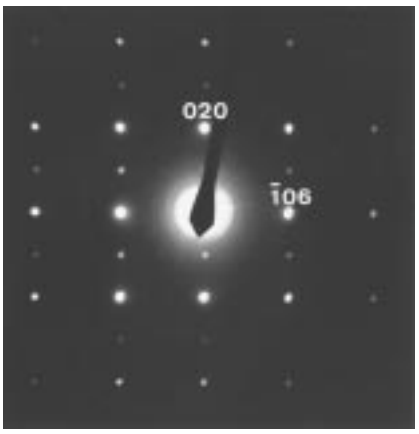

Fig. 5 Electron diffraction pattern along the $[60\bar{1}]$ zone axis of $Sr_2Bi_{1.4}Ca_{0.6}O_{5.21}$

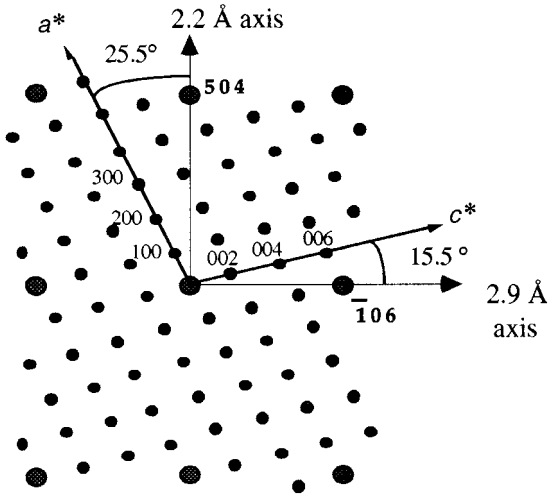

Fig. 6 Schematic diagram of the a^*c^* plane of $Sr_2Bi_{1.4}Ca_{0.6}O_{5.21}$ showing the relationship between the a^* and c^* axes and a perovskite subcell with $a=\sqrt{2}\ a_p$ and $c=a_p$

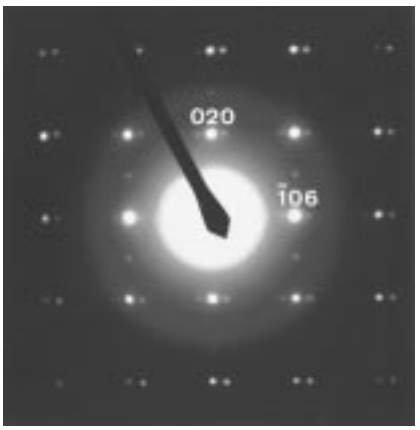

Fig. 7 Electron diffraction pattern along the $[110]_p$ zone axis of $Sr_2Bi_{1.4}Ca_{0.6}O_{4.70}$

According with TG experiments, the treatment of the reduced yellow phase $Sr_2Bi_{1.4}Ca_{0.6}O_{6-\delta}$ in oxygen at 650 °C for 36 h leads to a greenish black powder with an X-ray diffraction pattern that clearly corresponds to a perovskite structure [Fig. 1(*b*)]. This process appears to be reversible: the treatment in air or oxygen at 800 °C leads again to the yellow

phase:

$$\underset{\text{yellow}}{Sr_2Bi_{1.4}Ca_{0.6}O_{6-\delta}} + \delta/2O_2 \underset{800\,^{\circ}C,\ \text{air or } O_2}{\overset{O_2,650\,^{\circ}C}{\rightleftharpoons}} \underset{\text{black}}{Sr_2Bi_{1.4}Ca_{0.6}O_{6.0}}$$

The reduction of $Sr_2Bi_{1.4}Ca_{0.6}O_6$ in Ar–H_2 takes place in two separated steps (Fig. 8). The total mass loss is 9.25%, corresponding to an initial oxygen stoichiometry of 6.00 atoms per formula unit. Iodometric analysis of this sample leads to an oxygen content of 5.98 ± 0.05. The first mass loss (1.09%) occurs at low temperatures ($T_{onset} = 200\,^{\circ}C$) and leads to the stabilization of an intermediate phase with 5.60 O per formula unit. This process takes place also in Ar atmosphere, with identical mass loss at a similar temperature. The second step in Ar–H_2 corresponds to a mass loss of 8.16%, associated with the decomposition of this intermediate phase:

$$Sr_2Bi_{1.4}Ca_{0.6}O_{5.60} + 3H_2 \rightarrow 2SrO + 0.6CaO + 1.4Bi + 3H_2O$$

The formal oxidation state for bismuth in $Sr_2Bi_{1.4}Ca_{0.6}O_{6.00}$ is +4.85, corresponding to 7.5% of Bi^{3+} and 92.5% of Bi^{5+}. The phase with 5.60 O per formula unit was isolated by thermal treatment of $Sr_2Bi_{1.4}Ca_{0.6}O_{6.00}$ during 24 h at 300 °C in the furnace under an Ar flow. Despite the fact that this oxygen content is close to that of the yellow reduced phase, the colour of this sample is also greenish black and the corresponding X-ray diffraction pattern [see Fig. 1(*d*)] is similar to that of the oxidized phase $Sr_2Bi_{1.4}Ca_{0.6}O_{6.00}$.

The study of $Sr_2Bi_{1.4}Ca_{0.6}O_6$ by electron diffraction leads to an apparent orthorhombic cell with parameters $a = 5.9$, $b = 6.0$ and $c = 8.4$ Å (Fig. 9). These correspond to a perovskite with cell dimensions $\sqrt{2}\ a_p \times \sqrt{2}a_p \times 2a_p$. The observed reflection conditions $h0l$, $h+l=2n$, $h00$, $h=2n$, $00l$, $l=2n$ and $0k0$, $k=2n$ are consistent with the monoclinic space group $P2_1/n$ (no. 14). The spots $0k0$ with $k=2n+1$ in the patterns along the [100] and [001] zone axes are due to multiple reflections.

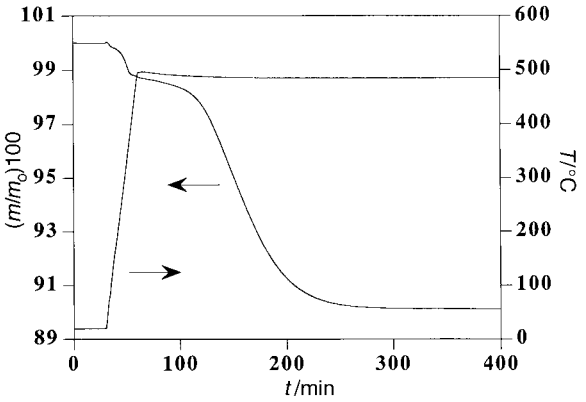

Fig. 8 TG plot in Ar–H_2 for $Sr_2Bi_{1.4}Ca_{0.6}O_6$

The electron diffraction planes for the phase with 5.60 O per formula unit obtained in Ar or Ar–H_2 are the same as for $Sr_2Bi_{1.4}Ca_{0.6}O_{6.00}$, suggesting a random distribution of the oxygen vacancies in the perovskite structure.

Crystal structure determination of $Sr_2Bi_{1.4}Ca_{0.6}O_6$

Fig. 10 shows the observed and calculated X-ray diffraction patterns and Table 1 gives the corresponding crystallographic data. A perspective view of the structure along a direction close to [110] ($[100]_p$) is shown in Fig. 11. The starting atomic coordinates for the profile refinement were taken from the perovskite La_2LiSbO_6, that shows the lattice constants $a = 5.6226(1)$, $b = 5.7199(1)$, $c = 7.9689(2)$ Å, $\beta = 89.796(9)^{\circ}$ and the same space group $P2_1/n$.[33] In this compound Li and Sb atoms are ordered in two B positions (2c and 2d) that alternate along the three crystallographic axes of the cubic perovskite subcell, in a NaCl-type distribution. La atoms occupy the A positions of the perovskite, all of them being crystallographically equivalent. In $Sr_2Bi_{1.4}Ca_{0.6}O_6$, the refinement was started with Bi and Ca occupying the two B sites and Sr in the A site, and a stoichiometry constraint was imposed in order to maintain the Bi to Ca ratio equal to that obtained from XEDS, 1.4–0.6 (an unconstrained refinement gave no significant deviations from these values). The final parameters for this model are shown in Table 1. These results were compared with those obtained starting with a model with one B position occupied statistically by Bi and Ca (site 4e) and two independent A sites for Sr atoms (sites 2c and 2d). The second model did not lead to a good fitting of the peak assigned to the reflection set 011, 101 and $10\bar{1}$ (2θ *ca.* 18°), very sensitive to the ordering of B cations (see inset on Fig. 10). This allowed us to accept the first model in which we refined different starting occupations for Bi and Ca in the two B sites. The best fitting corresponded to a model with site 1 (2c) occupied essentially by Bi (96%) and site 2 (2d) occupied by 45% of Bi and 55% of Ca, meaning that the B-cation arrangement is rock salt type and not random.

The two octahedra show metal–oxygen distances that agree with the mean ionic radii of each site, considering that 92.5% of bismuth is in +5 oxidation state ($r_{Bi^{5+}} = 0.74$ Å for CN = 6) (Table 2). The coordination polyhedron around Sr is a distorted cuboctahedron, showing eight M—O distances between 2.48 and 3.18 Å. Other bismuth alkaline earth perovskites showing ordering of B cations are $Ba_{2+x}Bi_{2-x}O_{6-\delta}$,[34] $Sr_{10}Bi_6O_{24-\delta}$, $Sr_6Bi_2O_{12-\delta}$[21] and $(Ba_{1-x}Sr_x)_2(Sr_{0.67}Bi_{0.33})(Pb_{1-y}Bi_y)O_{6-\delta}$.[22] The cationic order observed in such phases is similar to that of $Sr_2Bi_{1.4}Ca_{0.6}O_6$, with two sites, B and B′, alternating along the three directions, [100], [010] and [001] of the cubic perovskite subcell. However, the observed symmetry of those phases is higher than $P2_1/n$. They show rhombohedral, cubic, or tetragonal symmetries. The main

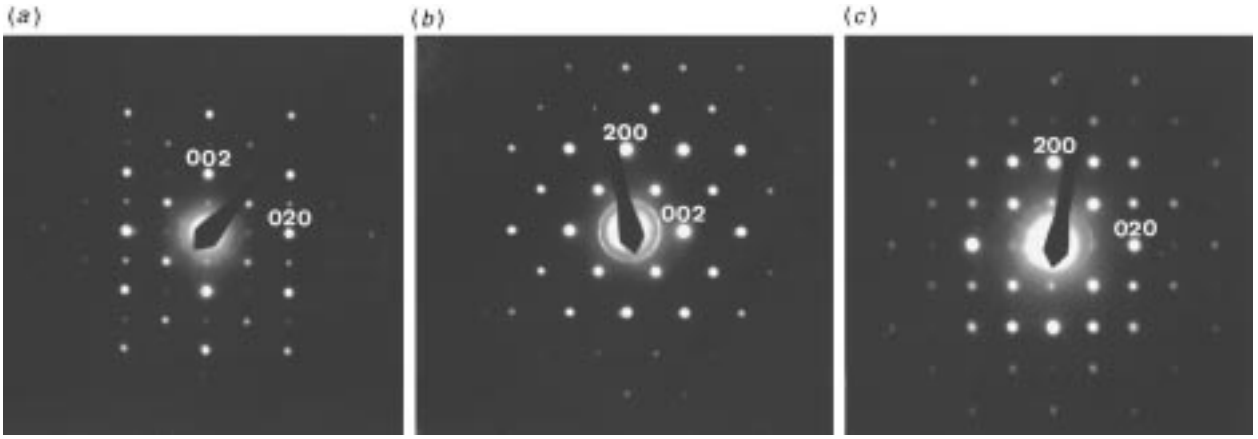

Fig. 9 Electron diffraction patterns corresponding to the [100] (*a*), [010] (*b*) and [001] (*c*) zone axes of $Sr_2Bi_{1.4}Ca_{0.6}O_{6.0}$

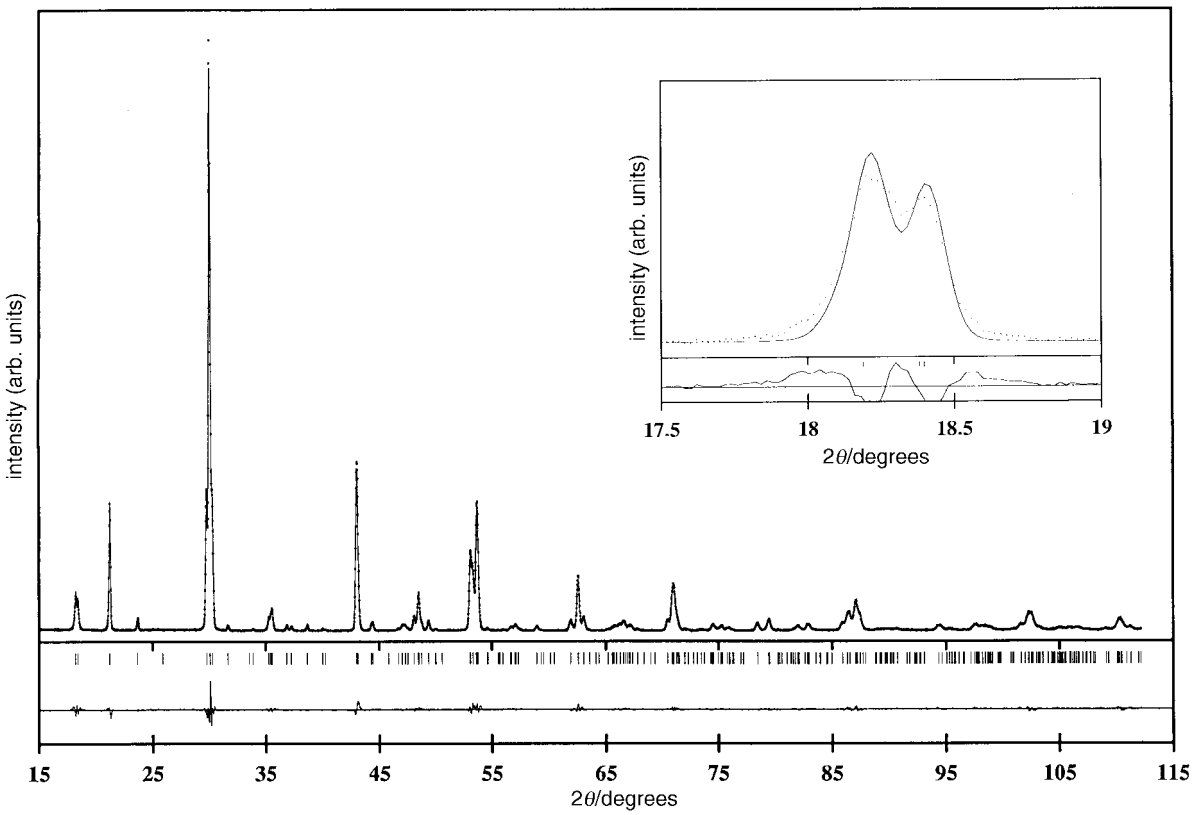

Fig. 10 Observed and calculated X-ray diffraction patterns for $Sr_2Bi_{1.4}Ca_{0.6}O_{6.0}$

Table 1 Crystallographic data for $Sr_2Bi_{1.4}Ca_{0.6}O_{6.0}$[a] (*a*) atomic coordinates and (*b*) thermal parameters

(*a*)

atom	*x*	*y*	*z*	occupancy factor	Wyckoff site symmetry
Bi(1)	0.0000	0.5000	0.0000	0.950(1)	2c
Ca(1)	0.00000	0.50000	0.0000	0.050(1)	2c
Bi(2)	0.5000	0.0000	0.0000	0.450(1)	2d
Ca(2)	0.5000	0.0000	0.0000	0.550(1)	2d
Sr	0.512(1)	0.5419(2)	0.2489(4)	1.0000	4e
O(1)	0.213(2)	0.218(2)	−0.070(2)	1.0000	4e
O(2)	0.287(2)	0.706(2)	−0.044(2)	1.0000	4e
O(3)	0.412(2)	0.969(1)	0.256(2)	1.0000	4e

(*b*)

	β_{11}	β_{22}	β_{33}	β_{12}	β_{13}	β_{23}
Bi/Ca(1)	32(6)	16(3)	−16(1)	−47(9)	−34(8)	10(9)
Bi/Ca(2)	51(11)	36(6)	9(2)	−46(15)	−92(12)	−12(15)
Sr	80(8)	75(6)	14(2)	13(12)	−49(11)	−18(7)

[a]Space group $P2_1/n$; $a=5.89228(9)$, $b=5.98928(8)$, $c=8.38336(14)$ Å, $\beta=89.946(5)^\circ$. Number of reflections = 411, $U=0.197(6)$, $V=-0.058(5)$, $W=0.0329(9)$. Reliability factors: $R_p=5.86$, $R_{wp}=8.19$, $R_e=5.00$, $\chi^2=2.69$, $R_{Brag}=2.86$. Thermal parameters ($\times 10^4$) according to the expression: $\exp[-h^2\ \beta_{11}+k^2\beta_{22}+l^2\beta_{33}+2hk\ \beta_{12}+2hl\ \beta_{13}+2kl\ \beta_{23})]$. β isotropic for O(1), O(2) and O(3) = 0.60(15) Å^2.

difference between those structures of similar topology and that of $Sr_2Bi_{1.4}Ca_{0.6}O_6$ comes from the different octahedral tilt system in each case. The cubic perovskites do not show such tilting (Glazer's[35] notation $a^0a^0a^0$), whereas $Sr_2Bi_{1.4}Ca_{0.6}O_6$ shows octahedral tilts in the three directions of the cubic perovskite subcell, $[100]_p$ (Glazer's notation: $a^-b^-b^-$).

Physical properties

Magnetic susceptibilities of oxidized and reduced samples with $x=0$, $Sr_2Bi_{1.4}Ca_{0.6}O_{6.0}$ and $Sr_2Bi_{1.4}Ca_{0.6}O_{5.21}$ were measured at 5 K for magnetic fields of 10, 100, 1000 and 10000 G. For all samples the observed values corresponded to the sum of atomic susceptibilities (between -600×10^{-6} and -200×10^{-6} emu mol^{-1}). The values for the room temperature electrical resistivities for the same samples were found in the range of megaohms.

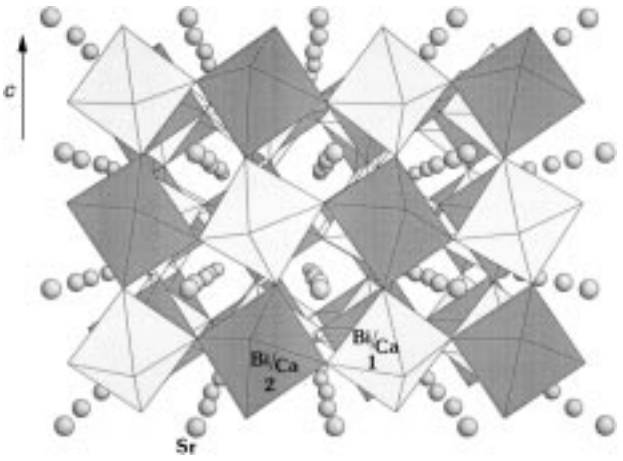

Fig. 11 Perspective view of the structure of $Sr_2Bi_{1.4}Ca_{0.6}O_{6.0}$ along a direction close to [110] ($[100]_p$)

Discussion

In bismuth perovskites, the reduction to oxygen deficient compounds containing Bi^{III} cations is commonly observed. Mixed valence and oxygen deficiency are related and have an influence on the crystal structure and properties. The temperature and atmosphere of the synthesis and annealing processes allow one to control the, frequently reversible, phase transitions or reactions involved. Moreover, for a given cationic stoichiometry, the structure of the final phase may be dependent upon the synthesis conditions.[13,22] This set of phenomena have

Table 2 Bond distances (Å) and angles (°) for $Sr_2Bi_{1.4}Ca_{0.6}O_6$

Bi/Ca(1)—O(1) (×2)	2.182(13)	Ca/Bi(2)—O(1) (×2)	2.220(13)
Bi/Ca(1)—O(2) (×2)	2.124(13)	Ca/Bi(2)—O(2) (×2)	2.195(13)
Bi/Ca(1)—O(3) (×2)	2.118(15)	Ca/Bi(2)—O(3) (×2)	2.216(15)
O(1)—Bi/Ca(1)—O(1)	180	O(1)—Ca/Bi(2)—O(1)	180
O(1)—Bi/Ca(1)—O(2)(×2)	86.9(8)	O(1)—Ca/Bi(2)—O(2)	89.5(8)
O(1)—Bi/Ca(1)—O(2)(×2)	93.1(9)	O(1)—Ca/Bi(2)—O(2)	90.5(8)
O(1)—Bi/Ca(1)—O(3)(×2)	93.0(1)	O(1)—Ca/Bi(2)—O(3)	97(1)
O(1)—Bi/Ca(1)—O(3)(×2)	87.0(8)	O(1)—Ca/Bi(2)—O(3)	82.7(8)
O(2)—Bi/Ca(1)—O(2)	180	O(2)—Ca/Bi(2)—O(2)	180
O(2)—Bi/Ca(1)—O(3)(×2)	91.2(1)	O(2)—Ca/Bi(2)—O(3)	87.9(9)
O(2)—Bi/Ca(1)—O(3)(×2)	88.8(9)	O(2)—Ca/Bi(2)—O(3)	92.1(9)
O(3)—Bi/Ca(1)—O(3)	180	O(3)—Ca/Bi(2)—O(3)	180
Sr—O(1)	2.476(16)	Sr—O(3)	2.630(9)
Sr—O(1)	2.634(16)	Sr—O(3)	2.533(12)
Sr—O(1)	2.961(17)	Sr…O(1)	3.747(16)
Sr—O(1)	3.181(16)	Sr…O(2)	3.642(16)
Sr—O(2)	2.814(16)	Sr…O(3)	3.479(12)
Sr—O(2)	2.560(16)	Sr…O(3)	3.425(11)
O(1)—Sr—O(1)	113(1)	O(2)—Sr—O(2)	126(1)
O(1)—Sr—O(2)	67.9(6)	O(2)—Sr—O(2)	117(1)
O(1)—Sr—O(2)	69.5(6)	O(2)—Sr—O(2)	126(1)
O(1)—Sr—O(2)	72.7(8)	O(2)—Sr—O(3)	66.1(6)
O(1)—Sr—O(2)	159(4)	O(2)—Sr—O(3)	66.5(6)
O(1)—Sr—O(2)	79.9(9)	O(2)—Sr—O(3)	133(1)
O(1)—Sr—O(2)	71.6(6)	O(2)—Sr—O(3)	110.2(9)
O(1)—Sr—O(3)	135(1)	O(2)—Sr—O(3)	65.9(5)
O(1)—Sr—O(3)	112(1)	O(2)—Sr—O(3)	132(1)
O(2)—Sr—O(2)	81.0(7)	O(3)—Sr—O(3)	86.9(5)

been already observed in the bismuth alkaline-earth oxides. Particularly the phase equilibria in the Bi–Sr–Ca–O system has been recently scrutinized.[24,25] In this context, two solid solutions, namely $Bi_9Sr_{11-x}Ca_{5+x}O_y$ and $Bi_2Sr_{1-x}Ca_{1+x}O_y$, have been identified. For the first of them a phase transition depending on the temperature and the oxygen partial pressure has been reported[24,25] and the reversibility of that process investigated.[23]

Roth *et al.* first reported a phase with stoichiometry $Sr_3CaBi_2O_7$ and parameters $a=20.000(8)$, $b=5.927(2)$, $c=11.283(4)$ Å and $\beta=101.68(3)°$.[36] It was described as a member of the solid solution $A_4Bi_2O_7$ (A=Sr,Ca) with a range of existence from Bi:Sr:Ca=3:2:1 to 5:6:4 [Bi/(Ca+Sr)=34/66]. Even though the cationic ratio of this phase is very close to $Sr_2Bi_{1.4}Ca_{0.6}O_{5.21}$, the oxygen content is different and corresponds to bismuth in +3 valence state. However, these authors did not mention the procedure followed to determine the oxygen stoichiometry. The reported space group was *C*2/*m*. We have synthesized some compositions of the formula $A_4Bi_2O_y$ and have found impurities under the electron microscope for all the samples, excluding $Sr_3CaBi_2O_y$. On the other hand, we were not able to distinguish among the electron diffraction planes of this sample and those of our phase $Sr_2Bi_{1.4}Ca_{0.6}O_{5.21}$. The two samples show the same space group, $P2_1/c$, and therefore we conclude that both are the same phase. On the basis of that result, the non-stoichiometry that we observed in the alkaline-earth ratio would extend to the bismuth composition and, consequently, a plausible alternative formula for the $Sr_3CaBi_2O_y$ compound would be $Sr_2Bi_{1.33}Ca_{0.66}O_y$. The thermal behaviour that we observe for $Sr_3CaBi_2O_y$ in Ar–H_2 and O_2 is nearly identical to $Sr_2Bi_{1.4}Ca_{0.6}O_{6-\delta}$. The oxygen stoichiometry is 7.76 atoms per formula unit, leading to an average formal oxidation state for bismuth of +3.76. The same authors later reported the existence of high and low temperature forms of that solid solution observed in samples with a Sr:Ca:Bi ratio of 49.5:16.5:34.0 (meaning $Sr_{2.044}Ca_{0.685}Bi_{1.4}O_y$).[24] The low (oxidized) temperature phase was then formulated as a triple perovskite structure with composition $(Sr_{2.97}Ca_{0.03})(Ca_{0.86}Bi^{3+}_{0.18}Bi^{5+}_{1.86})O_{8.88}$, space group *Pmmm* and lattice parameters $a=5.9979(3)$, $b=5.8966(3)$, $c=8.3907(4)$ Å. The high temperature (supposedly fully reduced to Bi^{3+}) form was analyzed by those authors as monoclinic with space group *Pc* and lattice parameters $a=11.224(1)$, $b=5.9064(5)$, $c=20.049(3)$ Å and $\beta=101.78(1)°$. An independent determination of the lattice parameters of that phase on samples with a Sr:Ca:Bi ratio of 35.3:28.7:36.0 (meaning $Sr_{1.37}Ca_{1.11}Bi_{1.4}O_y$), under the same hypothesis for the space group *Pc*, was recently published by Muller *et al.*[25] providing the set $a=11.195(2)$, $b=5.914(1)$, $c=19.972(4)$ Å and $\beta=101.78(1)°$. The stoichiometry range at 820 °C (35.2:28.8:36.0 to 54.7:9.3:36.0) determined under the stoichiometry restriction Bi/(Ca+Sr)=36/64, extends over the range found in our work to the region poorer in calcium. In fact our stoichiometry restriction [Bi/(Ca+Sr)=35/65] based on our structural characterisation of the oxidized, low temperature phase, was different to that proposed by Roth and Muller. No matter what the true stoichiometry may be, this phase is currently named 9$\underline{11}$5. The comparison of our results on the reduced and oxidized $(Sr_{2-x}Ca_x)(Bi_{1.4}Ca_{0.6})O_{6-\delta}$ solid solutions with those reported on the 9$\underline{11}$5 one shows that they must be in fact the same phases. Nevertheless significant discrepancies concerning the structural characterisation and also the stoichiometry of the system must be stressed.

Our X-ray diffraction work shows that the low temperature phase is an ordered double perovskite. It is a well established fact that, in $A_2BB'O_6$ perovskite oxides, ordering of the B-cation sublattice is energetically favoured *versus* random disorder as the charge (primarily) and size differences of the B cations increase. Nevertheless the maximum possible charge and ionic radius differences in $(Sr_{2-x}Ca_x)(Bi_{1.4}Ca_{0.6})O_6$ (*ca.* 1.99 and 0.18 Å, respectively) do not allow any prediction about the ordering scheme (on the established phenomenology)[37] for B cation arrangement in double perovskites. The cationic arrangement found by us in the $Sr_2Bi^{4.86+}_{1.4}Ca_{0.6}O_6$ crystal structure indicates that the mean charge on the two B sites is +3.15 and +4.85 respectively for the (2d) and (2c) sites, under the more plausible hypothesis that the Bi^{3+} atoms occupy exclusively the larger B sites (2d). The mean Bi—O bond distance at the (2d) and (2c) sites is 2.210 and 2.141 Å,

respectively. The mean distance for 2d sites agrees with the sum of ionic radii, considering 95% occupation of Bi^{5+} and 5% occupation of Ca.[38] In the 2c sites, the observed $Bi^{3+}-O$ bond distances are similar to those found by Cox and Sleight,[4] Thornton and Jacobson[5] or Chaillout *et al.*[39] in $BaBiO_3$.

Our space group determination for this phase by electron diffraction indicates monoclinic $P2_1/n$ as the only possibility, confirmed also through the observation of the reflection set (011,101 and $10\bar{1}$) around $2\theta = 18^\circ$ and the successful refinement of the structure. This group is, together with $Fm\bar{3}m$, one of the space groups observed in rocksalt ordered double perovskites. The cubic group $Fm\bar{3}m$ is observed with unit cells of type $2a_p \times 2a_p \times 2\ a_p$ in perovskites without octahedra tilting, whereas the monoclinic $P2_1/n$ has been observed in perovskites showing this tilting.[37] The allowed topological transformations of the perovskite structure, as outlined by Glazer,[35] do not allow the orthorhombic *Pmmm* space group proposed by Roth and co-workers for this phase.[24] The space group *Pc*, for the reduced (high temperature) phase has been proposed[24] through an (unpublished) single crystal X-ray diffraction analysis. Once again we disagree with these results. Our SAED study clearly shows that the true space group is centrosymmetric $P2_1/c$. The unit cell of the reduced phases obtained in air $(Sr_{2-x}Ca_x)(Bi_{1.4}Ca_{0.6})O_{6-\delta}$ ($\delta = 0.79$) is related metrically to that of those oxidized ones by the vectorial sums $\boldsymbol{a}_r = 1/2\ \boldsymbol{a}_o + 5/4\ \boldsymbol{c}_o$, $\boldsymbol{b}_r = \boldsymbol{b}_o$ and $\boldsymbol{c}_r = 3\boldsymbol{a}_o - \boldsymbol{c}_o$, subscripts r and o referring to the reduced and oxidized members. The establishment of this relationship did not allow us however to propose a plausible structural model for the reduced phases.[40] These show a large unit cell with high monoclinic distortion, and the oxygen stoichiometry corresponds to 63.6% of bismuth in +3 oxidation state. This cation shows very distorted and generally unpredictable coordination polyhedra with oxygen (coordination numbers from three to six). Because of that we are currently investigating the crystal structure of this phase by single crystal X-ray diffraction and high resolution electron microscopy.

The transformation from the reduced to the oxidized solid solutions depends on temperature and the oxygen partial pressure. As Baker and Glowacki have shown by consecutive nitrogen/oxygen annealing of the reduced phase up to 850 °C[23] on samples of stoichiometry $9\underline{11}5$, the redox process is probably reversible. This result agrees with our experiments. However we have observed that oxygen annealing processes of the same phase at higher temperatures (*ca.* 900 °C) do not yield a complete oxygen uptake to the oxidized form with $\delta = 0$. The latter is only obtained by oxygen processing at temperatures below 800 °C. These results, besides the observed differences in the allowed stoichiometry range for the reduced solid solution at 820 and 900 °C, suggest the occurrence of some irreversible processes at high temperatures. At low temperature these phases are very sensitive to atmospheric carbon dioxide or water and care must be taken in order to prevent analytical errors.

Despite the fact that the structure and bismuth valence of the reported phases are similar to those shown by K doped $BaBiO_3$, transport and magnetic properties of different members of the solid solutions do not show any superconducting or metallic behaviour. In the case of the oxidized phases, the reason must be the occupation of B positions by Ca in the perovskite structure, thus breaking the connectivity among bismuth ions present in the barium perovskite. Similar cation distribution has been observed in Ba_2BiO_4,[13] $Ba_{2+x}Bi_{2-x}O_{6-y}$[34] and $Sr_{10}Bi_6O_{24-y}$.[21] As in our case, those phases did not show superconductivity.

Conclusions

Two different phases around the BiSrCa $9\underline{11}5$ solid solution composition exist in the Bi–Sr–Ca–O quaternary system related by redox processes associated with phase transitions as shows the following scheme:

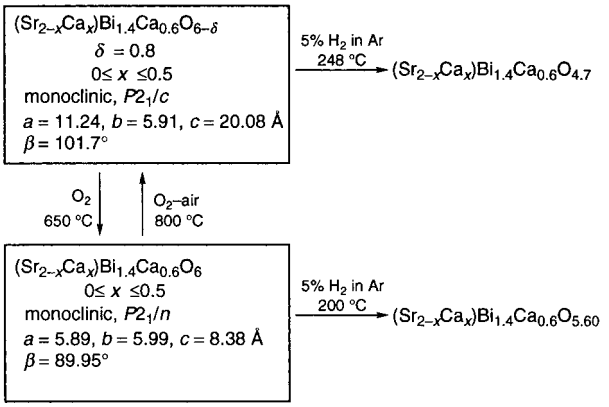

We have solved the crystal structure of the low-temperature (oxidized) phase showing that it is an ordered monoclinic $P2_1/n$ double perovskite corresponding to the structural formulation $Sr_2((Bi^{3+})_{0.098}Bi^{5+}{}_{0.352}Ca_{0.55}))(Bi^{5+}{}_{0.95}Ca_{0.05})O_6$. Thus, the right formulation for the oxidised $9\underline{11}5$ solid solution is $(Sr_{2-x}Ca_x)(Bi_{1.6}Ca_{0.4})O_6$. We have shown that the redox transition between the low and the high temperature phases occurs, at least, in the $0 \leqslant x \leqslant 0.5$ substitution range. For the reduced high temperature phase we have shown that the correct space group is $P2_1/c$ and the lattice shows a clear topological relationship with that of the perovskite oxidized one. The spreading of the Bi/(Sr + Ca) ratio (34/66, 35/65 and 36/64) observed by different authors in the reduced phase must be probably due to uncertainties inherent in experimental procedures. In any case the solid solution range in the pseudo-ternary Bi–Sr–Ca phase diagram seems to be one-dimensional. However from the precise analytical methodology used in our work we propose that the real Bi(Sr + Ca) ratio for the $9\underline{11}5$ solid solution must be very close to 35/65, that is 9/16.7 instead of 9/16 or 9/17.

The phases obtained by reduction in $Ar-H_2$ of the oxidized and reduced solid solutions are isostructural with the corresponding starting oxides. The phase with 4.7 O shows satellite reflections in some electron diffraction planes indicating the existence of a modulated superstructure. The phase with 5.60 O is obtained from the oxidized phase at very low temperatures ($T_{onset} = 200$ °C) through a reversible process, thus suggesting interesting applications as redox catalysts for these compounds.

This work has been funded by the Spanish CICYT (MAT93-0240-C04 and MAT96-1037-C02) and the Comissionat per Universitats I Recerca de la Generalitat de Catalunya (CIRIT). C.C.L. wants to thank a fellowship from the MUTIS program.

References

1 A. W. Sleight, J. L. Gillson and P. E. Bierstedt, *Solid State Commun.*, 1975, **17**, 27.
2 R. J. Cava, B. Batlogg, J. J. Krajewski, R. J. Farrow, L. W. J. Rupp, A. E. White, K. T. Short, W. F. J. Peck and T. V. Kometani, *Nature (London)*, 1988, **332**, 814.
3 R. J. Cava, in *Chemistry of Superconductor Materials. Preparation, Chemistry, Characterization and Theory*, ed. T. A. Vanderah, Noyes Publications, NJ, 1992, p. 380.
4 D. E. Cox and A. W. Sleight, *Solid State Commun.*, 1976, **19**, 969.
5 G. Thornton and A. J. Jacobson, *Acta Crystallogr., Sect. B*, 1978, **34**, 351.
6 J. G. Bednorz and K. A. Muller, *Z. Phys. B*, 1986, **64**, 189.
7 V. G. Wagner and H. Binder, *Z. Anorg. Allg. Chem.*, 1959, **298**, 12.
8 W. T. Fu, H. W. Zandbergen, Q. Xu, J. M. van Ruitenbeck, L. J. de Jongh and G. van Tendeloo, *Solid State Commun.*, 1989, **70**, 1117.
9 R. J. Cava, T. Siegrist, W. F. Peck, Jr., J. J. Krajewski, B. Batlogg and J. Rosamilia, *Phys. Rev. B*, 1991, **44**, 9746.
10 R. J. Cava, H. Takagi, H. W. Zandbergen, B. Hessen, J. J. Krajewski and W. F. Peck, Jr., *Phys. Rev. B*, 1992, **46**, 14101.

11 M. Licheron and F. Gervais, *J. Alloys Compd*., 1993, **195**, 77.
12 M. Licheron, F. Gervais, J. Coutures and J. Choisnet, *Solid State Commun*., 1990, **75**, 759.
13 K. P. Reis, A. J. Jacobson and J. Kulik, *Chem. Mater*., 1993, **5**, 1070.
14 F. Abbattista, M. Hervieu, M. Vallino, C. Michel and B. Raveau, *J. Solid State Chem*., 1993, **104**, 338.
15 A. Watanabe, *Solid State Ionics*, 1989, **35**, 281.
16 J. B. Parise, C. C. Torardi, C. J. Rawn, R. S. Roth, B. P. Burton and A. Santoro, *J. Solid State Chem*., 1993, **102**, 132.
17 I. Natali Sora, W. Wong-Ng, Q. Huang, R. S. Roth, C. J. Rawn, P. Burton and A. Santoro, *J. Solid State Chem*., 1994, **109**, 251.
18 J. B. Parise, C. C. Torardi, M.-H. Whangbo, C. J. Rawn, R. S. Roth and B. P. Burton, *Chem. Mater*., 1990, **2**, 454.
19 D. Conflat, J. C. Boivin, G. Tridot, *Comptes Rend. Seances Acad. Sci. Ser*., 1974, **279**, 457.
20 C. C. Torardi, J. B. Parise, A. Santoro, C. J. Rawn, R. S. Roth and B. P. Burton, *J. Solid State Chem*., 1991, **93**, 228.
21 Bokhimi and M. Portilla, *J. Solid State Chem*., 1993, **105**, 371.
22 C. Eylem, B. W. Eichhorn, Q. Huang and T. Clinton, *J. Solid State Chem*., 1995, **115**, 197.
23 A. P. Baker and B. A. Glowacki, *Physica C*, 1994, **223**, 383.
24 C. J. Rawn, R. S. Roth, B. P. Burton and M. D. Hill, *J. Am. Ceram. Soc*., 1994, **77**, 2173.
25 R. Müller, M. Cantoni and L. J. Gauckler, *Physica C*, 1995, **243**, 103.
26 G. Cliff and G. W. Lorimer, *J. Microsc*., 1975, **105**, 205.
27 A. K. Cheetham and A. J. Skarnulis, *Anal. Chem*., 1981, **53**, 1060.
28 J. Rodríguez-Carvajal, Program FULLPROF, Version 2.5, April 1994, ILL, unpublished.
29 A. Fuertes, C. Miravitlles, J. González-Calbet, M. Vallet-Regí, X. Obradors and J. Rodríguez Carvajal, *Physica C*, 1989, **157**, 525.
30 M. T. Caldés, J. M. Navarro, F. Pérez, M. Carrera, J. Fontcuberta, N. Casañ Pastor, C. Miravitlles, X. Obradors, J. Rodríguez Carvajal, J. M. González Calbet, M. Vallet Regí, A. García and A. Fuertes, *Chem. Mater*., 1991, **3**, 844.
31 M. T. Caldés, M. Hervieu, A. Fuertes and B. Raveau, *J. Solid State Chem*., 1992, **97**, 48.
32 *International Tables for X-Ray Crystallography*, ed. T. Hahn, Kluwer Academic Publishers, London, 3rd edn., 1992, vol. 1.
33 M. L. López, M. L. Veiga, J. Rodríguez-Carvajal, F. Fernández, A. Jerez, C. Pico, *Mater. Res. Bull*., 1992, **27**, 647.
34 K. P. Reis, A. J. Jacobson, J. M. Nicol, *J. Solid State Chem*., 1993, **107**, 428.
35 A. M. Glazer, *Acta Crystallogr*., *Sect. B*, 1972, **28**, 3384.
36 R. S. Roth, R. S. Burton and C. J. Rawn, *Ceramic Trans*., 1990, **13**, 23.
37 M. T. Anderson, K. B. Greenwood, G. A. Taylor and K. R. Poeppelmeier, *Prog. Solid State Chem*., 1993, **22**, 197.
38 R. D. Shannon, *Acta Crystallogr*., *Sect. A*, 1976, **32**, 751.
39 C. Chaillout, J. P. Remeika, A. Santoro and M. Marezio, *Solid State Commun*., 1985, **56**, 829.
40 C. C. Luhrs, Master Thesis, Universitat Autónoma de Barcelona, Bellaterra, October, 1995.

Paper 7/06160I; *Received* 15*th April*, 1997